Proceedings of the ASME 2009 International Design Engineering Technical Conferences &

Computers and Information in Engineering Conference

IDETC/CIE 2009

August 30 - September 2, 2009, San Diego, California, USA

DETC2009-86425

DRAFT: RABIT – RAPID AUTOMATED BIODOSIMETRY TOOL FOR HIGH THROUGHPUT RADIOLOGICAL TRIAGE

Youhua Chen[*]
Department of Mechanical Engineering

Jian Zhang
Department of Mechanical Engineering

Hongliang Wang
Department of Mechanical Engineering

Guy Garty
Center for Radiological Research

Yanping Xu
Center for Radiological Research

Oleksandra V. Lyulko
Center for Radiological Research

Helen Turner
Center for Radiological Research

Gerhard Randers-Pehrson
Center for Radiological Research

Nabil Simaan
Department of Mechanical Engineering

Y. Lawrence Yao
Department of Mechanical Engineering

D. J. Brenner
Center for Radiological Research

Advanced Robotics and Mechanism Applications Research Laboratory,
Columbia University, New York, NY 10027, U.S.A.

ABSTRACT

This paper presents design, hardware, software, and parameter optimization for a novel robotic automation system. RABiT is a Rapid Automated Biodosimetry Tool for high throughput radiological triage. The design considerations guiding the hardware and software architecture are presented with focus on methods of communication, ease of implementation, and need for real-time control V.S. soft time control cycles. The design and parameter determination for a non-contact PVC capillary laser cutting system is presented. A novel approach for lymphocyte concentration estimation based on computer vision is reported. Experimental evaluations of the system components validate the success of our prototype system in achieving a throughput of 6,000 samples in a period of 18 hours.

1 INTRODUCTION

The development of advanced methods for radiation biodosimetry is becoming a top priority need for the protection of environment and homeland security against possible radiological or nuclear attacks [1]. Even a dirty bomb in a large metropolitan area is likely to cause large scale panic, although the risk of radiological injuries is low. Because the general population would not carry physical dosimeters, a rapid method to assess an individual's radiation exposure is needed in such a situation.

In the past decade, many researchers have been working on designing a fully automated ultrahigh throughput biodosimetry system, based on robotic material handling and high speed imaging systems. Meldrum et al. demonstrated a capillary-based fluid handling system, ACAPELLA-5K (A5K), capable of processing genomic and chemical samples at a throughput of 5,000 preparations in 8 hours [2]. Kachel et al. designed a custom-made automated system capable of isolating DNA plasmids at a rate of 1,600 plasmids in 12 hours [3]. Prasanna et al. reported on the automation of cytogenetic biodosimetry featuring a throughput of 500 samples per week [4]. Soldatova et al. commissioned a new robotic system for investigations of gene function in capable of handling more than 1,000 samples a day [5].

This paper presents our ongoing efforts in the design, hardware and software integration, and experimental evaluation of a phase I high throughput biodosimetry system. The RABiT automates two mature, but currently manual, biodosimetry assays (micronucleus [8] [9] and γ-H2AX[10]), both of which have been shown to be highly radiation specific. The use of mature assays is critical for timely deployment,

[*] Post-doctor Research Scientist, Phone: (212) 854-7693, Fax: (212) 854-3304, Email: yc2491@columbia.edu.

because FDA pre-marketing requirements are much less time-consuming than for a new bio-assay. Lymphocytes, a type of white blood cells in human immune system, are extracted from blood samples into filter well plate through an automation system (Figure 1). The system consists of several modules: input stage, centrifuge, cell harvesting module, service robot, liquid/plate handling, incubator, high-speed imaging system, and central master controller.

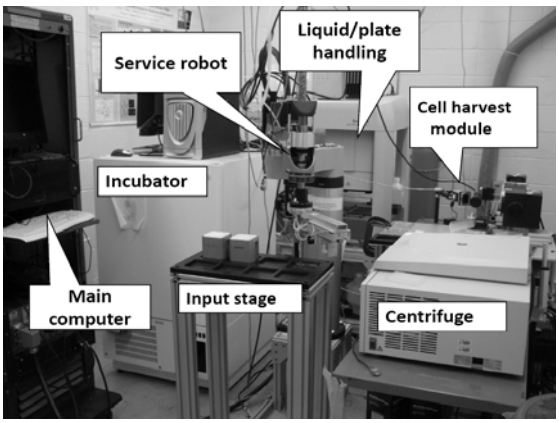

Figure 1. System breadboard prototype.

The blood samples are collected with a finger stick using a standard lancet (Figure 2a). The volume of each sample is 30µl. Blood is drawn into heparin-coated PVC capillary (RAM Scientific, Safe-T-Fill capillaries). The capillary is then loaded into a centrifuge bucket insert, prefilled with sealing putty and separation medium. The insert can be used for shipping the sample from the collection site to the RABiT where it is manually loaded into a centrifuge bucket on the input stage. Each bucket (Figure 2b) holds 3 inserts containing 32 capillaries each. For each time, four buckets are transferred from input stage (Figure 2c) to centrifuge (Figure 2d). After centrifugation at 4,000 rpm for 5 minutes, the lymphocytes are separated from Red Blood Cells (RBCs) (see Figure 2e). After PVC capillary laser cutting, the bottom part of the capillary with RBCs is disposed. The lymphocytes in the upper part are dispensed in a well plate (Figure 2f). Then after 72 hours incubation and staining, samples on filter bottoms of the well plate are transferred to imaging substrate and sealed (Figure 2g). Finally, the substrate is delivered to imaging module, where dedicated image hardware measures yields of micronuclei or γ-H2AXfoci, already well-characterized quantifiers for radiation exposure.

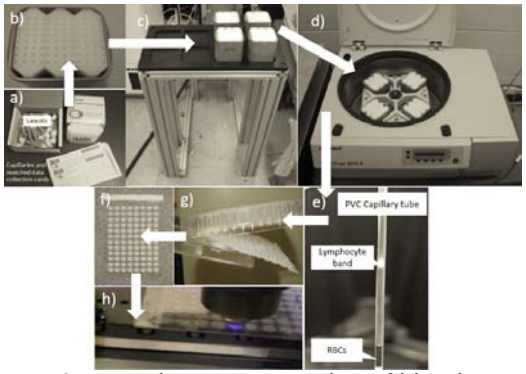

Figure 2. Lymphocyte separation of blood sample sequence.

The following sections present hardware design and implementation, software architecture and experimental performance validation of the system prototype.

2 HARDWARE AND IMPLEMENTATION

Figure 3 shows the three-tier hardware architecture of RABiT. The top tier is the central master controller. The middle tier includes all system components in direct communication with the central master controller. The bottom tier includes system peripherals controlled by secondary controllers of the equipments in the middle tier.

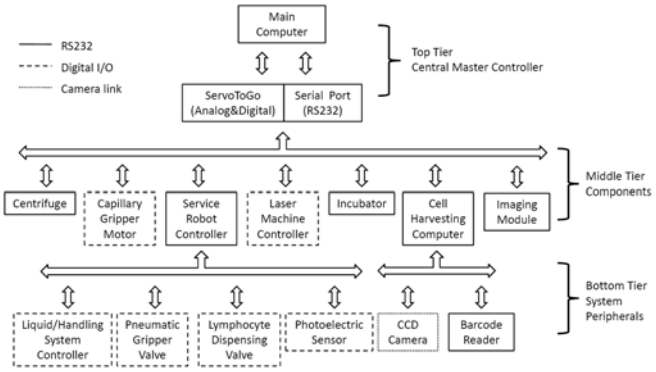

Figure 3. Hardware architecture.

The central master controller uses two types of communication protocols. One is based on the serial communication protocol, while the other is based on Digital & Analog I/O card (ServoToGo, ISA Bus Servo I/O Card Model 2). This I/O card has 32 bits of digital I/O, 8 channels of 13-bit analog input, and motion control ports for up to 8 differential TTL encoder signals.

The centrifuge (Eppendorf, 5810R) incorporates an interface board, a lid opener and a brake (Figure 4) such that through 5 bits of digital I/O, central master controller opener is able to take full robotic actions: open lid, load buckets, close lid, start centrifugation, stop centrifugation, open lid and unload buckets.

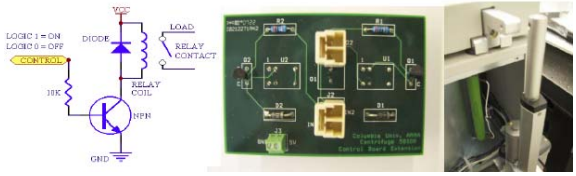

Figure 4. Electronic interface board and lid.

The PVC capillaries containing the separated blood are picked up by a customized gripper (Figure 5a). A multi-purpose pneumatic gripper (Figure 5b, SMC, MHF2-20D2) is used to pick, drop centrifuge buckets and well plates. The pneumatic gripper is controlled by a 4-way valve for air (Arozone, A212SS-O24-D-G 10197). The air pressure stays on 0.5MPa to achieve 12.1N of gripping force. The capillary gripper (Figure 5a) use a DC motor (Maxon, with a gear head and a 2-channel differential magnetic encoder) to control the rotation of its shaft. By one motion control channel of ServoToGo, the central master controller sets the reference voltage to the motor servo amplifier (Maxon, LSC30/2). Position feedback is implemented based on the encoder feedback at 1kHz.

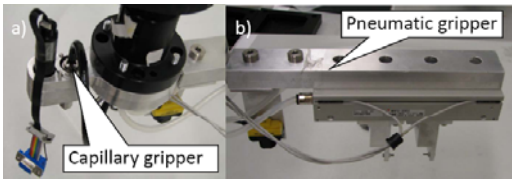

Figure 5. Multi-purpose material handling gripper.

The service robot (Staubli, RS80) communicates with its controller (Staubli, CS8C) by Can Bus. The central master controller always sends commands to the robot controller through a serial RS232 communication port. CS8C has 16 bits of digital input and 16 bits of digital output, which are used to control the peripheral devices that directly interface with the service robot (Figure 3). The liquid/handling system (CaliperLS, Sciclone ALH3000) takes 4 bits of digital input and 4 bits of digital output to communicate with the service robot such that robot can monitor the operation status of the Sciclone. Each of the pneumatic gripper valve and the lymphocyte dispensing valve take 1 bit of digital output from the robot controller CS8C based on digital I/O signals originating from the central master controller. Photoelectric sensor takes 1 bit of digital input used to detect the slot arm position in the centrifuge.

The communication between the central master controller and the laser machine uses RS232 serial communication. By sending character '1' or '0', the laser will turn the laser beam on or off. The parameters of the laser beam, such as laser power, and pulse frequency, are preset in the Windows-based controller of the laser machine.

The communication between the central master controller and the incubator is also based on RS232 protocol. After the central master controller sends a command to the incubator, the incubator will execute it and then send a status signal back to the central master controller. The central master controller can require the incubator to import or export a well plate, report its status, and read temperature/humidity of the incubator cabinet.

2.1 Cell Harvesting:

The cell harvesting module (Figure 6) processes incoming samples after centrifugation. Each PVC capillary is processed by this module with the purpose of extracting only the lymphocytes into a 96-well plate for subsequent liquid handling.

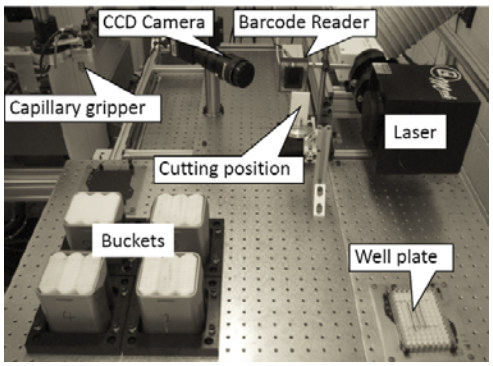

Figure 6. Cell harvesting module.

The cell harvesting module consists of a ultra-violet (UV) laser machine (Quantronix, Osprey-355-1-0), a barcode reader (Siemens, Hawkeye 1525HD), a CCD camera (JAI, CV-M4+CL), and custom-made holders for multi-well plates and centrifuge buckets.

Initially the servo robot picks centrifuged buckets from the centrifuge. Then the capillary gripper is used to pick up individual capillaries. As the diameter of the capillaries varies within a batch from 2.07mm to 2.16mm, the capillary gripper was designed to allow for variations in the diameter and achieved a successful picking of over 99% of the capillaries. This design implements a compliant rubber seal that accommodates diameter variation of the capillaries.

Figure 7. Barcode on the capillary.

The capillary is then moved into the field of view of the barcode reader for identification. Since the barcode etched on the capillary (Figure 7) is small (2.0mm×10.0mm), reliability of the barcode reader is important. However, repeating the reading process 3 times results in a success rate of 95% based on using code 128 for the barcode. After that, the capillary is moved into the field of view of the CCD camera. The CCD camera interfaces with the cell harvesting windows computer via a camera link connection and a frame grabber (NI, NI-1426) such that the cell harvesting computer is able to capture pictures and transfer the picture data quickly. Then imaging programs based on NI Vision will analyze the picture to detect the position of the separation band between the culture medium and the red blood cells.

In the following, the service robot moves down or up to align the separation band with the laser focal point. Then the robot sends 'ready' signal to the central master controller. The central master controller turns on the capillary gripper motor with 40rpm for 3.0s, and sends '1' to the laser machine to turn on the laser beam at the same time. After laser cutting, the bottom part with red blood cells drops in the disposing box. The upper part is positioned by the service robot above the well plate in order to dispense the lymphocytes in the well plate.

2.2 Laser Cutting:

The advanced UV laser is to realize non-contact cutting with the goal of eliminating cross-contamination among samples. The output power of the laser beam is 1.1W with 355nm wavelength, 20kHz pulse repetition frequency and 40μm of the effective spot size, thus the laser fluence is 4.377 J/cm^2. As to PVC absorption rate in [7], absorbed pulse energy of 266nm wavelengths is 18.33μJ, and the laser fluence at the focal plane becomes 1.46J/cm^2. Since the PVC ablation rate is 2.5μm/pulse [7], the thickness of the capillary is 0.5mm, so there should be at least 200 laser pulses of 0.01s duration to cut off the capillary. The corresponding rotation speed of the capillary gripper is 35.7rpm. This ensures circumferential cutting of the PVC capillaries. The optimal cutting time is 1.65 seconds.

The quality of laser cutting of PVC capillary tubes depends on the choice of effective parameters, including average laser power, motor rotation speed and cutting time. By analyzing the capillaries after cutting, such as change of inner diameter, outer diameter and thickness, dross attachment and

resolidification, and visible discoloration with burning, the cutting quality can be determined. Figure 8 shows the pictures of cross-sectional views of the sliced capillaries as seen under an optical microscope. The cutting quality under different power and rotation speeds are shown in Table1. The quality is classified from '0' to '5' with '0' designating worst and '5' presenting best cut quality. We can see that the optimal speed is 40rpm and the laser power is 0.8W. So the time of one-turn rotation is 1.5s. Since the ideal cutting time is 1.65s, we require the gripper motor to rotate two full turns to ensure full cutting of the capillary. Thus the cutting time used in our system is 3.0s per capillary.

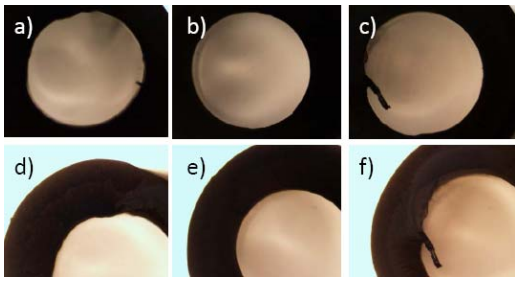

Figure 8. (a), (b) Cross-section views of capillary cut at 0.8W and 30rpm; (c), (d): 0.8W and 40rpm and (e), (f): 0.8W and 50rpm.

Table 1. Cutting quality.

	Power (W)						
Speed (rpm)		0.4	0.5	0.6	0.7	0.8	0.9
	30	0	2	2	2	3	0
	40	0	0	3	4	4	0
	50	0	0	0	3	3	3
	60	0	0	0	0	0	2
	65	0	0	0	0	0	3
	70	0	0	0	0	0	0

2.3 Lymphocyte Concentration Estimation:

Because the procedure of lymphocyte evaluation takes 72 hours for the γ-H2AXfoci protocol, it leads to the delay of treatment for severely irradiated patients. These patients should be treated as quickly as possible. The RABiT first triages incoming samples based on the concentration of the lymphocytes in centrifuged capillaries.

A novel, rapid quantitative light absorption analysis (QLAA) method has been developed to characterize lymphocyte concentration instead of quantitative buffy coat analysis (QBCA). The principle of light absorption in material is followed by Beer-Lambert Law. In experiment, we extracted the light absorption of lymphocytes by measuring the light transmittance of the separation medium and the separated lymphocytes, respectively.

Experiments tested the light absorption intensity calibration curves with different lymphocyte cells of whole blood (Figure 9). After blood separation, lymphocyte cells form a compact, high concentration band in capillary tube. In such case, light absorption analysis method is very useful to characterize the lymphocyte concentration. To determine the absolute lymphocyte cell number in the lymphocyte band and calibrate our system, we used a standard hemocytometer. The calibration curves have been extracted out based on the 30µl whole blood sample volume and 3000 lymphocyte cells per µl (compared to the 3000~10000cells/µl is the average range of fresh healthy human blood).

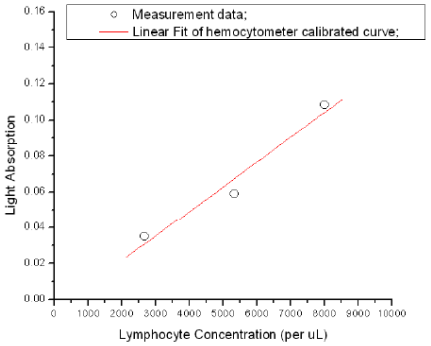

Figure 9. Lymphocyte calibration of light absorption.

2.4 Imaging Module:

After the lymphocytes are dispensed on the bottom of the well plate, the well plate is transferred to the liquid/plate handling system (CaliperLS, Sciclone ALH3000) and the incubator (Liconic, STX220) for 72-hour incubation and staining. In the following, the bottom substrate of the well plate is sealed and transferred to the imaging module. The high speed imaging module is developed to analyze the images of each assay in the sealed substrate to find the lymphocyte concentration. Figure 10 shows the imaging module. To meet the high throughput requirements, The RABiT imaging module incorporates three novel techniques for speeding up the imaging: use of light steering rather than sample motion, single-step auto-focusing and parallel use of multiple high-speed cameras.

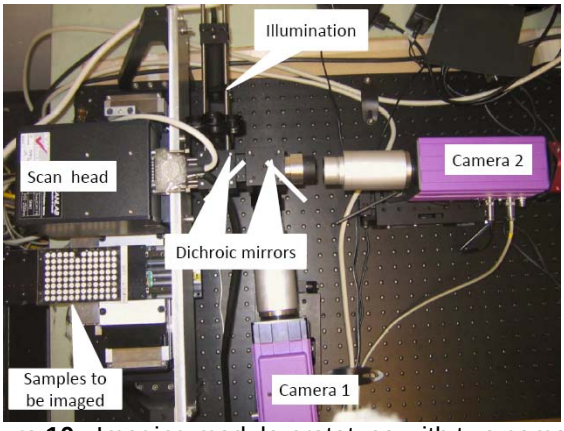

Figure 10. Imaging module prototype with two cameras for imaging DAPI and cell mask orange.

To achieve sufficient evaluation statistics, over one hundred 200-µm frames (fields of view) need to be imaged for each sample. Typically, imaging different frames within the same sample is achieved by mechanically moving the stage. However, mechanical motion takes tens of milliseconds, which is too slow. Instead of moving the sample, the light is steered into the camera using fast galvanometric mirrors. Typical transit times between adjacent fields of view are less than 1 msec.

One-step focusing is performed by incorporating an astigmatic element (a cylindrical lens) into one component of the optics. This results in a known focus-dependent distortion. For example, a spherical bead is imaged as an ellipse, and the aspect ratio of the ellipse indicates exactly how far the sample is out of focus. Figure 11 shows observed aspect ratio of a 4 μm fluorescent bead as a function of distance from focus using a cylindrical lens with a focal length of 500 mm.

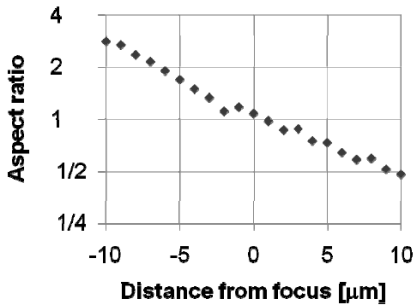

Figure 11. Observed aspect ratio.

Multiple cameras, sensitive to the colors of different dyes, allows simultaneous acquisition of separate images of the nucleus (stained using DAPI)and either the cytoplasm (stained using Cell Mask Orange) or γ-H2AXfoci (stained with Alexa fluor 555), as well as focus information.

3 SOFTWARE ARCHITECTURE

The RABiT system has three computers, and three machine controllers. Their operating systems and programming environments are listed in Table 2.

Table 2. System controller and programming.

Computer/Controller	*Operating System*	*Programming Tool*
Central master controller	Linux Fedora 8.0 with RTAI 3.6	GCC 4.1, Qt designer 4.4
Cell harvesting Computer	Windows XP	VC++ 2005
Service Robot Controller	Windows XP	VAL3, Staubli Robotic Studio 3.1
Laser Machine Controller	Windows XP	Quantronix DC2.2
Liquid/Handling System Controller	Windows XP	Sciclone Workstation 3.5
Imaging Module Computer	Windows XP	VC++ 2005

The central master controller is allocated for real-time application (kernel space) and non-real-time applications (user space). The classification of the system devices and their use of kernel space or user space memory are tabulated in Table 3. Real-time devices, for example, the capillary gripper motor, use 1kHz control loop frequency with closed-loop PID control. Non-real-time devices are instruments with a secondary dedicated controller where the application does not require a frequent real-time update of control reference signals.

Table 3. Device classification.

Device	*Real-time*	*Non-real-time*
Centrifuge	Yes	
Capillary Gripper Motor	Yes	
Service Robot Controller	Yes	
Laser Machine Controller		Yes
Incubator		Yes
Cell harvesting		Yes
Imaging module	Yes	

4 EXPERIMENTAL RESULTS

4.1 Throughput Analysis:

To meet the throughput requirements, we measured the time cost of the various steps of the capillary handling protocol shown in Figure 1. Table 4 is the time spent on each system modules. The total time for each sample is 11.06 sec, which means a throughput of 5859 samples in an 18-hour duty cycle.

Table 4. Completion times for major steps in the sample preparation protocol.

Step	*Time (sec)*	
	Total	*Per sample*
Load four buckets into centrifuge	97.5	0.25
Centrifugation	370	0.96
Unload centrifuge	52.8	0.14
Transfer one multi-well plate from stack to dispense position	6.8	0.07
Cell harvesting handling	9.64	9.64
Total time		11.06

The timing of the cell harvesting module takes 90% of the whole sample handling timing. Its sequential actions are pick one capillary, take a picture and locate lymphocyte band, move robot down to align the separation region between RBCs and separation medium in front of the laser, cut capillary, read barcode, dispense the lymphocyte, dispose of tube. Table 5 is the completion times of each action.

Table 5. Completion times of each action of cell harvesting.

Action	*Time (sec)*
Capillary picking	2.01
Imaging and cutting capillary	5.12
Lymphocyte dispensing and capillary disposing	2.51
Total time	9.64

4.2 Lymphocyte Concentration and Radiation Exposure Dose Evaluation:

Analysis of micronuclei and γ-H2AXfoci can be simplified to the detection of 'blobs and holes'. Assays can be simplified to the detection of 'blobs and holes', rather than more complex

morphometric structures, and thus the image analysis stages are very rapid. Analysis of the cytokinesis-block micronucleus assay is demonstrated in Figure 12. The raw images (Figure 12 a,b,d,e) are filtered and binarized, and a watershed algorithm is applied to separate touching objects. Then the two binary images (of nuclei and cytoplasms) are analyzed in conjunction with each other; the binarized image of the nuclei (Figure 12 a,d) is subtracted from the binarized image of the cytoplasms (Figure 12 b,e) and the nuclei belonging to each cell are identified in the subtracted image (Figure 12 c,f). The RABiT software then scores the number of micronuclei (small holes) in binucleated cells (those with two large holes). Thus, by the relation curve (Figure 13) between radiation exposure dose and micronuclei number, the radiation exposure dose will be evaluated.

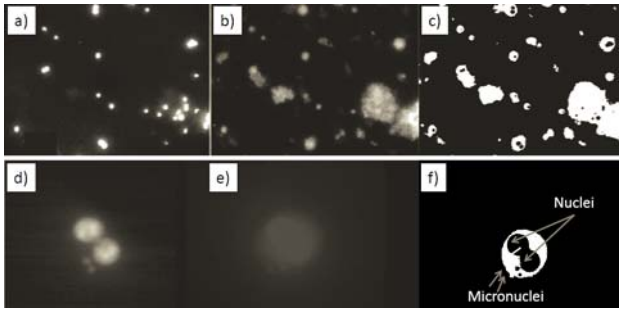

Figure 12. Sample image analysis

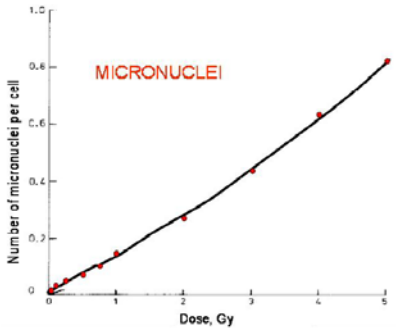

Figure 13. Radiation exposure dose calibration

5 CONCLUDING REMARKS

This paper reported the design, hardware, and software considerations for a Phase I robotic prototype of the high throughput bidosimetry system. This system integrates contactless laser machining, high-speed imaging, and custom-designed robotic components for a fully automated handling of incoming PVC capillaries. The experimental evaluation of this Phase I system shows its capability to process 5859 samples in an 18-hour duty cycle.

Future work is focused on increasing the throughput of this system by cutting down on the time delay during the various cell harvesting stages. Our efforts towards achieving these goals include optimized higher speed laser cutting of the PVC capillaries and integration of custom-designed robot for handling individual capillaries during the various stages of cell harvesting. This approach will allow parallel processing of samples during the cell harvesting stages.

6 ACKNOLEDGEMENTS

This work was supported by the NIH-funded Center for High-Throughput Minimally-Invasive Radiation Biodosimetry (NIAID Grant U19 AI067773).

7 REFERENCE

[1] T.C. Pellmar and S. Rockwell, Priority list of research areas for radiological nuclear threat countermeasures. Radiation Research, 2005. 163: p. 115-123.

[2] Meldrum, D.R., et al., Sample Preparation in Glass Capillaries for High-Throughput Biochemical Analyses, in International Conference on Automation Science and Engineering. 2005: Edmonton, Canada.

[3] V. Kachel, G.Sindelar, and S. Grimm, High-throughput isolation of ultra-pure plasmid DNA by a robotic system. BMC Biotechnology, 2006. 6(9).

[4] Prasanna, P.G.S., et al., Cytogenetic Biodosimetry for Radiation Disasters: Recent Advances. 2005, Technical Report. (AFRRI CD 05-2). Armed Forces Radiobiology Research Institute.

[5] Soldatova, L.N., et al., An ontology for a robot scientist. Bioinformatics, 2006. 22(14): p. 464-471.

[6] A. Salerno, J. Zhang, A. Bhatla, O. V. Lyulko, J. Nie, A. Dutta, G. Garty, N. Simaan, G. Randers-Pehrson, Y. L. Yao and D. J. Brenner. Design considerations for a minimally invasive high-throughput automation system for radiation biodosimetry. 3rd Annual IEEE Conference on Automation Science and Engineerin, 2007: p. 846-852.

[7] Mindaugas Gedvilas, Gediminas Račiukaitis. Investigation of UV picosecond laser ablation of polymers. Proc. of SPIE Vol. 6157, 61570T, 2005.

[8] Fenech, M., et al. HUMN project: detailed description of the scoring criteria for the cytokinesis-block micronucleus assay using isolated human lymphocyte cultures. Mutat Res 534, 2003:p. 65-75.

[9] IAEA. Cytogenetic analysis for radiation dose assessment: A manual, (International Atomic Energy Agency, Vienna, 2001).

[10] Nakamura, A., et al. Techniques for γ-H2AXdetection. Methods Enzymol 409, 2006:p. 236-250.